

Article

Distributed Control for Leader-Following Consensus Problem of Second-Order Multi-Agent Systems and Its Application to Motion Synchronization

Huaitao Shi *, Maxiao Hou and Yuhou Wu

College of Mechanical Engineering, Shenyang Jianzhu University, Shenyang 10153, China; houmax@stu.sjzu.edu.cn (M.H.); wuyh@sjzu.edu.cn (Y.W.)

* Correspondence: sht@sjzu.edu.cn; Tel.: +86-156-4235-5915

Received: 8 August 2019; Accepted: 2 October 2019; Published: 9 October 2019



Abstract: This paper solves the leader-following consensus problem for a class of second-order multi-agent systems with input quantized by a newly proposed adaptive dynamic quantizer. The novel dynamic quantizer is an adaptive quantizer that combines the logarithmic quantizer and the uniform quantizer by introducing dynamic gain parameters to achieve quantizer adaptive adjustment. It has advantages of logarithmic, uniform, and adaptive dynamic quantizers in ensuring reducible communication expenses and acceptable quantizer errors for better system performance. On this basis, we transform the guide way climbing frame (GWCF) under ideal conditions into a second-order multi-agent system and solve the motion synchronization problem of GWCF. Finally, we illustrate our approach by numerical examples.

Keywords: second-order multi-agent systems; adaptive dynamic quantizer; consensus; motion synchronization; distributed control law

1. Introduction

Because of cooperative control widespread potential applications in various fields such as synchronized rise of guide way climbing frame (GWCF), formation control of mobile robots, distributed coordination of multiple dynamic systems (also known as multi-agent systems [1–6]), has achieved rapid development in recent decades. Consensus is one of the most popular topics in this area, which has received significant attention from numerous researchers [7,8]. These approaches are often classified as leaderless consensus [9–11] and leader-following consensus solutions (see [12–14] and the references therein). Moreover, many of the early works were established for systems with first-order dynamics, whereas more results have been reported in recent years, such as [15] for systems with second or higher-order dynamics.

However, all the above results assume that the communication among the agents under consideration is not limited [16,17], and that real-time changes are entered in the context of continuous time. This assumption does not hold in practical systems, and mechanical equipment cannot be adjusted in real time under continuous-time conditions. Therefore, the consensus problem under the limitation of communication bandwidth [18,19] has become a new hot-spot issue in the field of control. In recent years, most consensus problems have been solved in the background of dynamic discrete time [20,21]. However, the practical system is rare in the context of dynamic discrete time. It is more in the context of continuous time, so it is very meaningful to solve the consensus problem of bandwidth limitation in a continuous-time background. Therefore, this paper uses the quantization approach to solve the bandwidth limitation or finite capacity problem in continuous-time dynamics. Quantization can be seen as a map from continuous signals to discrete finite sets [22]. Quantizer digitizes incoming

information and usually gives piecewise constant output and input. Therefore, only finite bits of channel capacity are required for the transmission of quantized data among agents [23,24]. To our best knowledge, the current research on the consensus of multi-agent systems under input quantization is not very extensive.

Static quantizer include logarithmic quantizer and uniform quantizer, which usually contains a fixed quantization interval and an infinite quantization level. Compared with newly proposed adaptive dynamic quantizer, it is inefficient and unrealistic. When the input of system is large, the use of logarithmic quantizer will lead to large quantization error, which makes the system instability. When the input of system is small, the use of uniform quantizer also will lead to relatively large quantization error. To overcome the shortcomings of two static quantizers, which are static and have large errors under specific conditions, the newly proposed adaptive dynamic quantizer combines the logarithmic quantizer and the uniform quantizer by introducing dynamic gain parameters, and gives the boundary conditions. The error of the newly proposed adaptive dynamic quantizer is less than that of the dynamic uniform quantizer [25] when the input of system is small, and which is equal to that of the dynamic uniform quantizer when the input of system is large. Generally speaking, the quantization error of this quantizer has dynamic quantization interval, limited quantization level and small quantization error compared with the logarithmic quantizer [26], uniform quantizer [27] and dynamic uniform quantizer.

To our best knowledge, dynamic uniform quantizer has been applied to leaderless multi-agent systems. For systems with information quantization, input is quantized by a quantizer which results in an inevitable quantization error. Because when an actual value is sent from an agent to its neighbor, the value will be truncated and only a quantified version will be received by the neighbor, which may cause undesirable oscillating behavior in the process of leader-following consensus [28,29]. Therefore, it is still very challenging to consider the leader-following consensus of multi-agent systems under followers input quantization. In fact, many practical systems that can be transformed to second-order multi-agent systems, such as synchronous motion of GWCF. In this paper, the followers' input are quantized by the newly proposed adaptive dynamic quantizer, which solve the problem leader-following consensus with limited communication bandwidth. The static quantizer in [30] is a special case of the newly proposed dynamic quantizer, the dynamic gain parameter is 1 and applied to the SISO system [31].

At present, the synchronous motion of the second-order system has not been resolved very well. For example, the synchronized rise of GWCF adopts switches for one-to-one control of each node. During the lifting process, there are four observers around. When the GWCF in that direction rises and falls, slowly or quickly, the switches of corresponding nodes are controlled by the indoor personnel through the walkie-talkie. It makes the whole rises process very inefficient and the workload of the staff is huge. To effectively solve this problem and be more suitable for practical working conditions, we adopt the distributed control law. This law cannot only make current node state within a reasonable range according to the state of the around nodes, but also require a small number of calculations by a single node. To apply the distributed control law, we first build the mathematical model by analyzing the force on the practical object, and then calculate it, such as the vertical force of each hanging point in the climbing frame, the horizontal force of a single mobile robot and so on, under the condition that the friction force does not changed by the time. A mathematical model of a second-order integrator systems is established for the longitudinal force of the single hanging point in the GWCF. The second-order integrator system of all hanging points constitutes a network structure, which is regarded as a second-order multi-agent systems. Supposing one of the hanging point with constant speed is the leader, the other hanging points are the followers. The pull of the motor at a single suspension point is the input to a single second-order integrator system. Under the action of a novel adaptive dynamic quantizer, the input of a single hanging point can be adjusted intermittently in the initial stage of the motion process by means of distributed control law, and the synchronous motion can be achieved in a short time.

In this paper, we first introduce self-proposed adaptive dynamic quantizer which has dynamic quantization interval, limited quantization level and smaller quantization error compared with the logarithmic quantizer, uniform quantizer and dynamic uniform quantizer. On this basis, the follower input is quantized by a dynamic quantizer in a second-order integrator multi-agent systems, and the leader-following consensus problem with limited communication bandwidth is solved by a distributed control law. Finally, the distributed control law is applied to practical systems, such as synchronous motion of GWCF. According to the simulation example, the better results are achieved.

The main contributions of this paper include three aspects.

(1) First, a novel adaptive dynamic quantizer is proposed. Compared with the previous quantizer, this quantizer can effectively reduce quantization error, has dynamic quantization interval and limited quantization level.

(2) Secondly, most of researcher solve the multi-agent system consensus problem after the input is quantized, using leaderless method and the quantizer adopts the static quantizer. In this paper, using second-order systems and having a leader, the problem of leader-following consensus of multi-agent systems is realized by using the adaptive dynamic quantizer proposed by ourselves. The second-order system and the self-proposed adaptive dynamic quantizer are more realistic.

(3) Moreover, the mathematical model of the second-order multi-agent system is established by analyzing the vertical force acting on the lifting nodes of GWCF under ideal conditions. The second-order multi-agent system will realize synchronous lifting of GWCF under the distributed control law whose input is quantized by the novel adaptive dynamic quantizer.

The rest of the paper is organized as follows. In Section 2, we will give the basic notion and preliminary results. In Section 3, we will give the problem statement. In Section 4, we will give the main result and stability analysis. The effectiveness of the proposed method and design is illustrated by examples in Section 5. Some concluding remarks are given in Section 6. In addition, some proofs are attached in the Appendix A.

2. Basic Notions and Preliminary Results

In this section, we introduce graph theory, some basic concepts of quantizers, and propose a novel dynamic quantizer.

2.1. Graph and Matrix

We first introduce some graph terminologies which can be found in [32]. A digraph $g = (v, \epsilon)$ consists of finite set of nodes $v = \{1, 2, 3, \dots, N\}$ and an edge set $\epsilon \subseteq v \times v$. An edge of ϵ from node i to node j is denoted by (i, j) , where the nodes i and j are called the parent node and child node of each other, and the node i is also called a neighbor of the node j . Let N_i denote the subset of v which consists of all the neighbors of node i . If the digraph g contains a sequence of edges of the form $(i_1, i_2), (i_2, i_3), \dots, (i_k, i_{k+1})$, then the set $\{(i_1, i_2), (i_2, i_3), \dots, (i_k, i_{k+1})\}$ is called a path of g from node i_1 to node i_{k+1} and node i_{k+1} is said to be reachable from node i_1 . if $i_1 = i_{k+1}$, the path is called a cycle. The adjacency matrix of g is defined as $A_g = [a_{ij}] \in R^{N \times N}$ with nonnegative adjacency elements $a_{ij} > 0 \Leftrightarrow (j, i) \in \epsilon$. The degree matrix $\Delta_g = [\Delta_{ij}]$ is a diagonal matrix with $[\Delta_{ii}] = \sum_{j=1}^N a_{ij}$, $i = 1, 2, \dots, N$, element and the graph Laplacian of the weighted digraph g is defined by $L = \Delta_g - A_g$ whose eigenvalues will be ordered and denoted as $0 < \lambda_1 \leq \lambda_2 \leq \dots \leq \lambda_N$. L corresponding eigenvector $1 = [1, 1, \dots, 1]^T$, i.e., $L1 = 0$.

Lemma 1 ([33]). *For a quasi-strongly connected graph g , the graph Laplacian L have the N nonzero eigenvalues, which are all in the open right-half plane.*

2.2. Quantizer Description

2.2.1. Logarithmic Quantizer

In this section, the logarithmic quantizer described in [34] is considered. The quantizer with bounded region satisfies the following properties:

$$q_l(u) = \begin{cases} u_i & \frac{u_i}{1+\delta} < u < \frac{u_i}{1-\delta} \\ 0 & 0 \leq u < \frac{d}{1+\delta} \\ -q_l(-u) & u < 0 \end{cases} \quad (1)$$

$$|\Delta q_l(u)| \leq \delta|u| + (1 - \delta)d \quad (2)$$

where $\Delta q_l(u) = q(u) - u$, q_l with quantization error Δq_l , $u_i = \rho^{(1-i)d}$, $i = 1, 2, \dots, N$. The parameters $d > 0$ and $0 < \rho < 1$, $\delta = \frac{1-\rho}{1+\rho}$ determine the quantization density of $q_l(u)$. $q_l(u)$ is in the set $U = \{0, \pm u_i\}$. $u_{min} = \frac{d}{1+\delta}$ determines the size of the deadzone for $q_l(u)$. For this quantizer, some remarks about its range, number of quantization levels and quantization density are given in [35].

2.2.2. Hysteresis Quantizer

The hysteresis quantizer employed is described in the following form, similar to [36].

$$q_h(u) = \begin{cases} u_i \text{sgn}(u) & \frac{u_i}{1+\delta} < |u| < u_i, \dot{u} < 0, \text{ or} \\ & u_i < |u| \leq \frac{u_i}{1-\delta}, \dot{u} > 0 \\ u_i(1+\delta) \text{sgn}(u) & u_i < |u| \leq \frac{u_i}{1-\delta}, \dot{u} < 0, \text{ or} \\ & \frac{u_i}{1-\delta} < |u| \leq \frac{u_i(1+\delta)}{1-\delta}, \dot{u} > 0 \\ 0 & 0 \leq |u| < \frac{d}{1+\delta}, \dot{u} < 0, \text{ or} \\ & \frac{d}{1+\delta} \leq |u| \leq d, \dot{u} > 0 \\ q(u(t^-)) & \dot{u} = 0 \end{cases} \quad (3)$$

where $i = 1, 2, \dots, N$, the parameters $d > 0$ and $0 < \rho < 1$ determine the quantization density of $q(u)$, $\delta = \frac{1-\rho}{1+\rho}$, $u_i = \rho^{1-i}d$. $q(u)$ is in the set $U = \{0, \pm u_i, \pm u_i(1 + \delta)\}$ and $q(u(t^-))$ denotes the status prior to $q(u(t))$. For this kind of quantizer, some detailed discussions about its parameters and hysteresis mechanism can be found in [35].

The hysteresis quantizer can be considered to be an extension of the logarithmic quantizer, it can be seen as a combination of two logarithmic quantizers with the same coarseness but different quantized values. Thus, control law, which adopts a logarithmic quantizer, can be also applied to the hysteresis quantizer, and vice versa. In the rest part of the paper, we only consider the logarithmic quantizer for simplicity. However, with the additional quantized values, a hysteresis quantizer can avoid chattering phenomenon. The detailed discussions can be found in [37].

2.2.3. Uniform Quantizer

The uniform quantizer was proposed in [38], which had relatively simple form and was described as

$$q_u(u) = \left\lfloor \frac{u}{\omega} + \frac{1}{2} \right\rfloor \omega \quad (4)$$

where $\lfloor a \rfloor$ denotes the greatest integer, it is less than or equal to a , ω is the parameter ($\omega > 0$) of the uniform quantizer, which can be found in [38]. For this kind of quantizer, the following inequality is satisfied.

$$|\Delta q_u(u)| \leq \frac{1}{2}\omega. \tag{5}$$

where the quantization error of q_u is Δq_u , the logarithmic quantizer and the hysteresis quantizer satisfy property with $0 < \delta < 1$ based on [39]. For the uniform quantizer, the sector bound property is also true with $\delta = 0$ and $d = \frac{\omega}{2}$.

2.2.4. Novel Adaptive Dynamic Quantizer

For a logarithmic quantizer, the quantization level becomes coarser as the magnitude of signal gets larger (away from the original), the uniform quantizer has the disadvantage of fixed error that the error does not decrease when the input is very small, dynamic uniform quantizer is no exception. To overcome these problems, we propose a novel adaptive dynamic quantizer, which combines the logarithmic quantizer and the uniform quantizer by introducing dynamic gain parameters, give the boundary conditions of the novel quantizer. (Please note that this quantizer can be easily extended to a combination of a hysteresis quantizer and a uniform quantizer by replacing $q_l(\cdot)$ with $q_h(\cdot)$).

$$kq_\chi(u/k) = \begin{cases} kq_l(u_{th}) + \left\lfloor \frac{u - ku_{th}}{k\omega} + K \right\rfloor k\omega & ku_{th} \leq u \leq kM \\ kq_l(\frac{u}{k}) & 0 < u < ku_{th} \\ -kq_\chi(\frac{-u}{k}) & u < 0 \end{cases} \tag{6}$$

where $kq_\chi(u/k)$ is the result of quantization of novel adaptive dynamic quantizer, k is the constant to be specified later, $k(k > 0)$ is adopted as a zooming variable, kM is quantization range. $K = \frac{1}{2}$, if $q_l(u_{th}) < u_{th}$ and $K = 0$ if $q_l(u_{th}) \geq u_{th}$, u_{th} is a positive constant specified by the designer denoting the threshold to switch between the dynamic logarithmic quantizer and dynamic uniform quantizer, the equation $\frac{1}{2}\omega = |q_l(u_{th}) - u_{th}|$, where ω is a parameter for the dynamic uniform quantizer.

Let us make $k = 1$, $\omega = 1$. We get Figure 1.

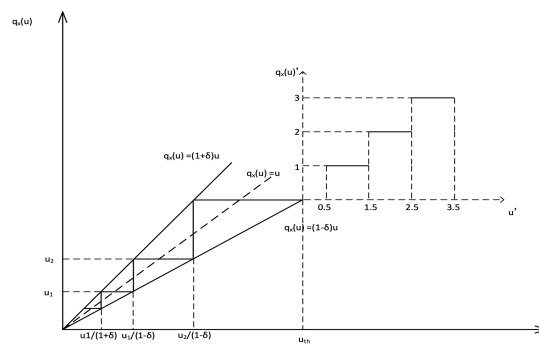


Figure 1. Novel adaptive dynamic quantizer.

Remark 1. The quantization error of the novel adaptive dynamic quantizer is shown below (see the proof in Appendix A).

$$|\Delta q_\chi(u)| \leq \begin{cases} k(\delta \frac{|u|}{k} + (1 - \delta)d) & |u| < ku_{th} \\ \frac{1}{2}k\omega & ku_{th} \leq |u| \leq kM \end{cases} \tag{7}$$

where $d > 0$, $0 < \rho < 1$, $\delta = \frac{1-\rho}{1+\rho}$, the quantization error of $kq_\chi(\frac{|u|}{k})$ is Δq_χ , Δq_χ for the novel adaptive dynamic quantizer is always bounded for any u . In addition, low communication cost is still maintained with a suitable choice of large u_{th} . Thus, the newly proposed adaptive dynamic quantizer has the advantages of logarithmic, uniform, dynamic uniform quantizers.

The quantization error comparisons of magnitude between the newly proposed adaptive dynamic quantizer and the traditional dynamic uniform quantizer as follows:

According to (7), we divide the input into the following three stages to analyze.

$$\begin{cases} \Delta q_\mu = \Delta q_\chi = \frac{1}{2}k\omega & |u| > ku_{th} \\ \Delta q_\mu = \Delta q_\chi = \frac{1}{2}k\omega & |u| = ku_{th} \\ \Delta q_\chi < \Delta q_\mu & |u| < ku_{th} \end{cases}$$

where Δq_μ is the quantization error of the dynamic uniform quantizer mentioned in [25], $\Delta q_\chi = k(\delta \frac{|u|}{k} + (1 - \delta)d)$, $\frac{d\Delta q_\chi}{du} > 0$.

In summary, the error of the dynamic uniform quantizer is Δq_μ , the error of the newly proposed adaptive dynamic quantizer is Δq_χ . $\Delta q_\mu \geq \Delta q_\chi$ if the input is in a finite compact set, it will be more clearly illustrated by the subsequent digital simulation.

3. Problem Statement

Considering the GWCF, we can write the equation of motion in the vertical direction as

$$\begin{aligned} F_i(t) - f_i - m_i g - m_i \ddot{x}_i(t) &= 0 \\ f_i &= \mu_i N_i \quad i = 1, \dots, N \end{aligned} \tag{8}$$

$F_i(t)$ represents the pulling force of each hanging point, μ_i is the coefficient of sliding friction of an object at each hanging point, N_i is the pressure on the orbit of the object at each hanging point, f_i is the sliding friction force in the vertical direction of an object at each hanging point, m_i is the mass of an object at each hanging point, g is the acceleration of gravity. To obtain the state space model of the GWCF synchronized rise. First, let us take the state variables as $x_{1i} = x_i(t)$ and $x_{2i} = \dot{x}_i(t)$. Then the state space equation of the input quantized is as follows by the newly proposed adaptive quantizer (6)

$$\dot{x}_{1i} = x_{2i} \tag{9}$$

$$\dot{x}_{2i} = kq_\chi \left(\frac{u_i}{k} \right) \tag{10}$$

where $u_i = \frac{F_i}{m_i} - \frac{f_i}{m_i} - g$, $i = 1, \dots, N$, $x_{1i} = \text{col}(x_{11}(t), \dots, x_{1N}(t))$, $x_{2i} = \text{col}(x_{21}(t), \dots, x_{2N}(t))$ is the state, $u_i = u_i(t)$ is the input.

$$\dot{x}_{10} = x_{20} \tag{11}$$

$$\dot{x}_{20} = u_0 \tag{12}$$

where $x_{10} \in R$ and $x_{20} \in R$ are an exogenous signal, $x_{10} = x_{10}(t)$, $x_{20} = x_{20}(t)$, $u_0 = u_0(t)$.

The plants (9), (10) and the exosystems (11), (12) together can be viewed as multi-agent systems of $N + 1$ agents with (11), (12) as the leader and the N subsystems of (9), (10) as N followers. Given the plant (9), (10), the exosystem (11), (12), we can define a digraph $g = (v, \epsilon)$.

To describe our control law, denote the adjacency matrix of digraph g by $A = [a_{ij}] \in R^{(N+1) \times (N+1)}$ where $a_{ii} = 0$, $a_{ij} = 1 \Leftrightarrow (j, i) \in \epsilon$, and $a_{ij} = 0 \Leftrightarrow (j, i) \notin \epsilon$ for $i, j = 0, 1, \dots, N$. According to the paper [25], we can get the following control law:

$$u_i = - \sum_{j=0}^N a_{ij}(x_{1i} - x_{1j}) - \sum_{j=0}^N a_{ij}(x_{2i} - x_{2j}) \tag{13}$$

where $i = 0, \dots, N$, the control law of the form (13) is called distributed control law. It can only access to the information of its neighbors and itself.

Our problem is described as follows:

Problem 1. Given the multi-agent system (9)–(12) under the distributed control law (13), the state of followers eventually tends to leader’s state by using the newly proposed adaptive dynamic quantization, i.e., $\lim_{t \rightarrow \infty} |x_{1i} - x_{10}| = 0$, $\lim_{t \rightarrow \infty} |x_{2i} - x_{20}| = 0$, $i = 1, \dots, N$.

The structure of the system quantization method is shown in Figure 2.

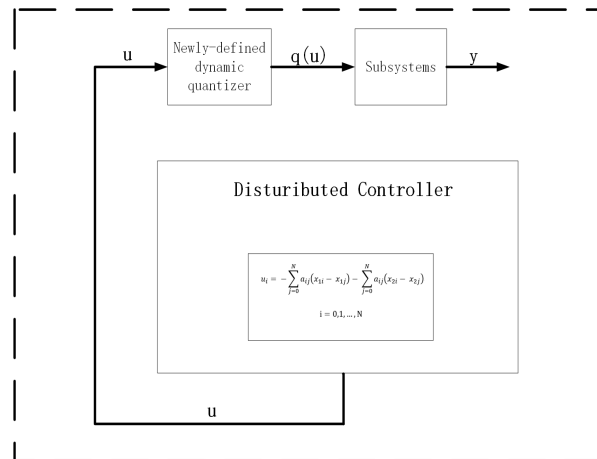


Figure 2. Subsystem quantization method.

Following the framework in [40], for a given plant to stabilization problem of a well-defined augmented system, we will first convert the leader-following consensus problem of multi-agent systems.

$$\bar{x}_{1i} = x_{1i} - x_{10}; \tag{14}$$

$$\bar{x}_{2i} = x_{2i} - x_{20}; \tag{15}$$

where $i \in 1, \dots, N$. Then, according to (9)–(15) we can get the following form:

$$\dot{\bar{z}} = A\bar{z} + Be \tag{16}$$

where matrix A and matrix B are Hurwitz, A is Laplacian matrix, according to Laplacian property we get x_{1i} and x_{2i} to receive signals from itself and its neighbor (that is, only nodes near the leader can accept the leader’s information), $e = e_i$ is quantization error, the specific values of matrix A , B and e are introduced later. $\bar{z} = \bar{z}_i = \begin{bmatrix} \bar{x}_{1i} \\ \bar{x}_{2i} \end{bmatrix}$, $i = 1, \dots, N$. If the closed-loop system (16) admits Lyapunov functions $U_p(\bar{z}_i)$, satisfying

$$\tilde{a}_1(\|\bar{z}_i\|) \leq U_p(\bar{z}_i) \leq \tilde{a}_2(\|\bar{z}_i\|) \tag{17}$$

$$\frac{\partial U_p}{\partial t} \leq -\lambda_0 U_p(\bar{z}_i) \tag{18}$$

where $i = 1, \dots, N$, for some class k_∞ functions $\tilde{a}_1(\cdot)$ and $\tilde{a}_2(\cdot)$, and some positive number λ_0 , then origin of (16) is globally asymptotically stable.

4. Main Result and Stability Analysis

In this section, we will consider stabilization problem for the system (16). For this purpose, according to (6), (9), (10) and (13), we first propose the following equation:

$$\begin{aligned} \ddot{x}_{1i} &= kq_\chi \left(\frac{-\sum_{j=0}^N a_{ij}(x_{1i}-x_{1j}) - \sum_{j=0}^N a_{ij}(x_{2i}-x_{2j})}{k} \right) \\ &= -kq_\chi \left(\frac{Lx_{1i}}{k} + \frac{Lx_{2i}}{k} \right) \\ &= -Lx_{1i} - Lx_{2i} - e_i \end{aligned} \tag{19}$$

According to (19), (9) and (10) is converted into following form:

$$\begin{bmatrix} \dot{x}_1 \\ \dot{x}_2 \end{bmatrix} = \begin{bmatrix} 0 & I \\ -L & -L \end{bmatrix} \begin{bmatrix} x_{1i} \\ x_{2i} \end{bmatrix} - \begin{bmatrix} 0 \\ 1 \end{bmatrix} (e_i) \tag{20}$$

where $e_i = kq_\chi \left(\frac{Lx_{1i}}{k} + \frac{Lx_{2i}}{k} \right) - (Lx_{1i} + Lx_{2i})$, $\hat{L} = \begin{bmatrix} 0 & I \\ -L & -L \end{bmatrix}$, $x_{1i} = x_{1i}(t)$, $x_{2i} = x_{2i}(t)$, $i = 1, \dots, N$.

We translate (9), (10) into the following form:

$$\dot{x}_{1i} = x_{2i} \tag{21}$$

$$\dot{x}_{2i} = -Lx_{1i} - Lx_{2i} - e_i \tag{22}$$

then define the following T, T^+ (see the solution process in Appendix A) and \hat{T}^+ matrix:

$$T = \begin{bmatrix} -1 & 1 & 0 & \cdots & 0 \\ -1 & 0 & 1 & \cdots & 0 \\ \vdots & \vdots & \vdots & \ddots & \vdots \\ -1 & 0 & 0 & \cdots & 1 \end{bmatrix}$$

$$T^+ = \begin{bmatrix} -\frac{1}{N} & -\frac{1}{N} & -\frac{1}{N} & \cdots & -\frac{1}{N} \\ \frac{N-1}{N} & -\frac{1}{N} & -\frac{1}{N} & \cdots & -\frac{1}{N} \\ -\frac{1}{N} & -\frac{N-1}{N} & -\frac{1}{N} & \cdots & -\frac{1}{N} \\ \vdots & \vdots & \vdots & \ddots & \vdots \\ -\frac{1}{N} & -\frac{1}{N} & -\frac{1}{N} & \cdots & \frac{N-1}{N} \end{bmatrix}$$

$$\hat{T}^+ = \begin{bmatrix} T^+ & 0 \\ 0 & T^+ \end{bmatrix}$$

where $T \in R^{N \times (N+1)}$, $T^+ \in R^{(N+1) \times N}$ and $\hat{T}^+ \in R^{2(N+1) \times 2N}$.

According to T , we translate (14) and (15) into the following equations:

$$\bar{x}_{1i} = Tx_{1i} \tag{23}$$

$$\bar{x}_{2i} = Tx_{2i} \tag{24}$$

where $i \in 1, \dots, N, \iota \in 0, \dots, N$.

For convenience of writing, we translate (23), (24) into the following equation:

$$\bar{z} = \hat{T}z \tag{25}$$

where $z = z(t) = \begin{bmatrix} x_{1i} \\ x_{2i} \end{bmatrix}$, $\bar{z} = \bar{z}(t) = \begin{bmatrix} \bar{x}_{1i} \\ \bar{x}_{2i} \end{bmatrix}$, $\hat{T} = \begin{bmatrix} T & 0 \\ 0 & T \end{bmatrix}$, $i = 1, \dots, N$.

According to (14) and (15), (19) is converted into the following form:

$$\begin{aligned}
 \ddot{\bar{x}}_{1i} &= T\ddot{x}_{1i} \\
 &= -TLx_{1i} - TLx_{2i} - Te_i \\
 &= -TLT^+\bar{x}_{1i} - TLT^+\bar{x}_{2i} - Te_i \\
 &= -\bar{L}\bar{x}_{1i} - \bar{L}\bar{x}_{2i} - Te_i
 \end{aligned}
 \tag{26}$$

where $\bar{L} = TLT^+, e = e_i, i = 1, \dots, N, i = 0, \dots, N$.

According to (14) and (15), (20) is converted into the following form:

$$\begin{bmatrix} \dot{\bar{x}}_1 \\ \dot{\bar{x}}_2 \end{bmatrix} = \begin{bmatrix} 0 & I \\ -\bar{L} & -\bar{L} \end{bmatrix} \begin{bmatrix} \bar{x}_1 \\ \bar{x}_2 \end{bmatrix} - \begin{bmatrix} 0 \\ T \end{bmatrix} (e)
 \tag{27}$$

where

$$\bar{L} = \begin{bmatrix} l_{11} - l_{01} & l_{12} - l_{02} & \cdots & l_{1n} - l_{0n} \\ l_{21} - l_{01} & l_{22} - l_{02} & \cdots & l_{2n} - l_{0n} \\ \vdots & \vdots & \ddots & \vdots \\ l_{n1} - l_{01} & l_{n2} - l_{02} & \cdots & l_{nn} - l_{0n} \end{bmatrix}$$

We get following equation:

$$\dot{\bar{z}} = \check{L}\bar{z} - \check{E}e
 \tag{28}$$

where $x_1 = x_{1i}, x_2 = x_{2i}, \check{L} = \begin{bmatrix} 0 & I \\ -\bar{L} & -\bar{L} \end{bmatrix}, \check{E} = \begin{bmatrix} 0 \\ T \end{bmatrix}, \check{L} \in R^{2N \times 2N}, \check{E} \in R^{2N \times (N+1)}, \bar{z} = \begin{bmatrix} \bar{x}_1 \\ \bar{x}_2 \end{bmatrix},$

$A = \check{L}, B = \check{E}$.

According to (7), The quantization error $|e|$ of the novel adaptive dynamic quantizer is as follows:

$$|e| \leq \begin{cases} (\delta \frac{|U|}{k} + (1 - \delta)d)k & |U| < kx_{th} \\ \frac{1}{2}k\omega & kx_{th} \leq |U| \leq kM \end{cases}
 \tag{29}$$

where $U = U_i = Lx_{1i} + Lx_{2i}, i = 0, \dots, 1, k \in N^+, kM$ is the maximum quantization range, kx_{th} is the switching value of dynamic logarithmic quantizer and dynamic uniform quantizer in a novel adaptive dynamic quantizer. The parameters $d(d > 0)$ and $\rho(0 < \rho < 1), \delta(\delta = \frac{1-\rho}{1+\rho})$ determines the size of the deadzone for $q_i(u)$. Where $[a]$ denotes the greatest integer that is less than or equal to $a, \omega(\omega > 0)$ is the parameter of uniform quantizer and determines the quantization density. We defined $\frac{1}{2}k\omega = kq_i(x_{th}) - kx_{th}$. where $q_i(\cdot)$ is the logarithmic quantizer.

Theorem 1. *The leader-following consensus problem of system (9)–(12) is transformed into the problem of augment system (16) origin stabilization. We can solve Problem 1, i.e., get the following equation:*

$$\lim_{t \rightarrow \infty} \bar{z} = 0
 \tag{30}$$

Proof. We can define the nonsingular special P matrix.

$$P = \begin{bmatrix} \rho & 0 \\ 0 & \rho \end{bmatrix}
 \tag{31}$$

where $\rho = \begin{bmatrix} T \\ \frac{1}{\sqrt{N}}\mathbf{1}^T \end{bmatrix}, \mathbf{1} = [1, 1, \dots, 1]^T$. The inverse matrix of the P matrix is shown below:

$$P^{-1} = \begin{bmatrix} \rho^{-1} & 0 \\ 0 & \rho^{-1} \end{bmatrix}
 \tag{32}$$

Clearly the eigenvalues of $P\hat{L}P^+$ are same as those of \hat{L} , we have

$$\begin{aligned}
 P\hat{L}P^{-1} &= \begin{bmatrix} 0 & 0 & I & 0 \\ 0 & 0 & \dots & 0 \\ -TLLT^+ & \vdots & -TLLT^+ & \vdots \\ 0 & 0 & \cdot & 0 \end{bmatrix} \\
 &= \begin{bmatrix} 0 & 0 & I & 0 \\ 0 & 0 & \dots & 0 \\ -\bar{L} & \vdots & -\bar{L} & \vdots \\ 0 & 0 & \cdot & 0 \end{bmatrix}
 \end{aligned}
 \tag{33}$$

The eigenvalues of (33) are the solutions of the characteristic polynomial.

$$\det(\lambda I - P\hat{L}P^{-1}) = \lambda^2 \det(\lambda I - \check{L}) = 0
 \tag{34}$$

Therefore \check{L} has the same eigenvalues of \hat{L} but the two zero eigenvalue.

The existence of negative definite matrix τ makes positive definite matrix symmetric matrix η and θ to satisfy the following equation:

$$\tau^T \eta + \eta \tau = -\theta
 \tag{35}$$

We can choose following Lyapunov function candidate.

$$v = \bar{z}^T \eta \bar{z}
 \tag{36}$$

where $v = v(t)$, $\lambda_{min}(\eta)$ and $\lambda_{max}(\eta)$ are some know class K_∞ functions, and they are the smallest and largest eigenvalues of matrix η , respectively.

$$\lambda_{min}(\eta) |\bar{z}|^2 \leq v \leq \lambda_{max}(\eta) |\bar{z}|^2
 \tag{37}$$

According to (28), By taking the derivate of (36), we get the following inequality:

$$\begin{aligned}
 \dot{v} &\leq -\bar{z}^T \theta \bar{z} - 2\bar{z}^T \eta \check{E} e \\
 &\leq -\lambda_{min}(\theta) |\bar{z}|^2 + 2|\bar{z}^T \eta \check{E} e| \\
 &= -\lambda_{min}(\theta) |\bar{z}| (|\bar{z}| - \frac{2\|\eta \check{E} e\|}{\lambda_{min}(\theta)})
 \end{aligned}
 \tag{38}$$

According to Equation (29), e is a piecewise function, so we get the following inequality:

$$\begin{aligned}
 \dot{v} &\leq \min(-\lambda_{min}(\theta) |\bar{z}| (|\bar{z}| - \frac{\|\eta \check{E}\| |k\omega| \sqrt{M}}{\lambda_{min}(\theta)}), \\
 &-\lambda_{min}(\theta) |\bar{z}| (|\bar{z}| - \frac{2\|\eta \check{E}\| (\delta \frac{|U|}{k} + (1-\delta)d)k \sqrt{M}}{\lambda_{min}(\theta)}))
 \end{aligned}
 \tag{39}$$

We replace the variables in (39) for facilitate writing as follows:

$$\phi = \begin{cases} \frac{\|\eta \check{E}\| |k\omega| \sqrt{M}}{\lambda_{min}(\theta)} & kM \geq |U| \geq kx_{th} \\ \frac{2\|\eta \check{E}\| (\delta \frac{|U|}{k} + (1-\delta)d)k \sqrt{M}}{\lambda_{min}(\theta)} & |U| < kx_{th} \end{cases}
 \tag{40}$$

According (7), we get $\phi_{max} = \frac{\|\eta \check{E}\| |k\omega| \sqrt{M}}{\lambda_{min}(\theta)}$.

So that for any $\epsilon > 0$, we get the following piecewise function:

$$\phi_{max} \leq (1 + \epsilon) \phi_{max} \leq |\bar{z}|
 \tag{41}$$

Under the condition of (41), we obtain the inequality $\dot{v} < 0$, and transform the inequality of (38) into the following form:

$$\dot{v} \leq -\lambda_{\min}(\theta) \left(\frac{\epsilon}{1+\epsilon}\right) \frac{v}{\lambda_{\max}(\eta)} \tag{42}$$

We replace the following variable for facilitate writing:

$$a = \frac{\lambda_{\min}(\theta)}{\lambda_{\max}(\eta)} \frac{\epsilon}{1+\epsilon} \tag{43}$$

Then by applying the Comparison Lemma [39], we can provide the following estimates of the convergence rate as in [40].

$$\dot{v} \leq -av \tag{44}$$

By solving (44) inequality, we get the following answer:

$$v \leq e^{-at}v(0) \tag{45}$$

Based on Lemma 1 of [41], for an arbitrary $\epsilon > 0$, we according to different definitions can define the ellipsoid.

$$\begin{cases} R_1 := \{\bar{z} : \lambda(\eta)|\bar{z}|^2 \leq \lambda_{\min}(\eta)k^2M^2\} \\ R_2 := \{\bar{z} : \lambda(\eta)|\bar{z}|^2 \leq \lambda_{\max}(\eta)((1+\epsilon)\phi_{\max})^2\} \end{cases} \tag{46}$$

According to (46), R_1 and R_2 are invariant regions for the multi-agent system (28). With this setting, the trajectories of (28) starting in R_1 will approach R_2 in finite time.

We can provide the estimates (44) of the convergence rate as in [35]. With the estimation of the upper bound of the convergence time that starting in R_1 enter R_2 as

$$\psi = \frac{1}{a} \ln \frac{\lambda_{\min}(\eta)(M)^2}{\lambda_{\max}(\eta)(1+\epsilon)^2\phi_{\max}^2} \tag{47}$$

To guarantee the asymptotic stability of the whole system, the Liberzon’s design strategy [41] is employed. The control scheme contains two steps: “zooming-out” to detect measurement of states by increasing k ; “zooming-in” to achieve more accurate quantization by decreasing k . When the initial state is in ellipsoid R_1 or R_2 with the initial zooming variable $k(t_0)$, the zooming-in phase starts with the update interval ψ . Let $k(t) = k(t_0)$ for $t \in [t_0, t_0 + \psi]$, where ψ is given by (47). Then $\bar{z}(t_0 + \psi)$ belongs to the ellipsoid R_1 . The equation about k is as follows:

$$k = \pi^\beta k_0 \tag{48}$$

$$\pi = \frac{\sqrt{\lambda_{\max}(\eta)(1+\epsilon)\phi_{\max}}}{\sqrt{\lambda_{\min}(\eta)M}} \tag{49}$$

where $k = k(t)$, $k_0 = k_0(t)$, ψ is defined as (47) and β is the number of update times. It is easy to check $\pi < 1$ and $k < k_0$ according to (48) and (49). To decrease k by means of multiplying it by the scaling factor π , we have $\lim_{t \rightarrow \infty} k = 0$, (44) implies $\lim_{t \rightarrow \infty} \bar{z} = 0$. \square

Remark 2. As the initial states of multi-agent systems generally known for quantizers, we can select $k_0 < 1$ in advance to keep the systems starts in the ellipsoids R_1 (46).

Remark 3. The steps for proof $\lim_{t \rightarrow \infty} \bar{z}(t) = 0$ under novel dynamic quantizer, are summarized as follows:

- (1) Design the novel dynamic quantizer (6) as shown in Section 2.

(2) The design transforms the multi-agent consensus problem into the origin stabilization problem in Section 3.

(3) Lyapunov function are defined in (36) and prove that in Section 4.

5. Example

In this section, a simulation example is provided for illustration. We consider the form of the second-order integrator multi-agent system with followers state quantized by the newly proposed adaptive dynamic quantizer is as follows. The exosystem is in the form of (11), (12).

$$\begin{aligned} \dot{x}_{1i} &= x_{2i} \\ \dot{x}_{2i} &= q_\chi\left(\frac{F_i}{m_i} - \frac{f_i}{m_i} - g\right) \end{aligned} \tag{50}$$

where $u_0 = 0$. $q_\chi(\cdot)$ is the state quantization by quantizer (1), where $d = 0.02, \delta = 0.2, x_{th} = 14, \omega = 0.84$. The initial quantization parameter is k_0 , so that the initial condition after transformation is in ellipse R_1 (46). Reduction ratio π and update interval ψ are calculated by (47), (49).

A network of three followers is modeled by (50), which is shown in the Figure 3. where node 0 represents the exogenous signal (leader) and other nodes represent followers.

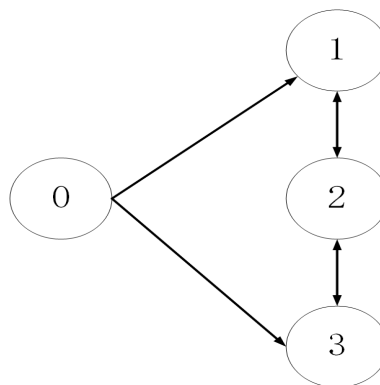


Figure 3. The communication graph.

$$\hat{L} = \begin{bmatrix} 0 & 0 & 0 & 0 & 1 & 0 & 0 & 0 \\ 0 & 0 & 0 & 0 & 0 & 1 & 0 & 0 \\ 0 & 0 & 0 & 0 & 0 & 0 & 1 & 0 \\ 0 & 0 & 0 & 0 & 0 & 0 & 0 & 1 \\ 0 & 0 & 0 & 0 & 0 & 0 & 0 & 0 \\ 1 & -2 & 1 & 0 & 1 & -2 & 1 & 0 \\ 0 & 1 & -2 & 1 & 0 & 1 & -2 & 1 \\ 1 & 0 & 1 & -2 & 1 & 0 & 1 & -2 \end{bmatrix}$$

where L is the Laplacian matrix after conversion of adjacent matrix.

$$\check{L} = \begin{bmatrix} 0 & 0 & 0 & 1 & 0 & 0 \\ 0 & 0 & 0 & 0 & 1 & 0 \\ 0 & 0 & 0 & 0 & 0 & 1 \\ -2 & 1 & 0 & -2 & 1 & 0 \\ 1 & -2 & 1 & 1 & -2 & 1 \\ 0 & 1 & -2 & 0 & 1 & -2 \end{bmatrix}$$

where $-\check{L}$ is Hurwitz, the matrix η and θ are calculated by linear matrix inequality $\theta = -\check{L}\eta - \eta\check{L}^T$, obtain as follows:

$$\eta = \begin{bmatrix} 3.9375 & 2.25 & 1.3125 & -1.5 & 0 & 0 \\ 2.25 & 5.25 & 2.25 & 0 & -1.5 & 0 \\ 1.3125 & 2.25 & 3.9375 & 0 & 0 & -1.5 \\ -1.5 & 0 & 0 & 2.625 & 0.75 & 0.375 \\ 0 & -1.5 & 0 & 0.75 & 3 & 0.75 \\ 0 & 0 & -1.5 & 0.375 & 0.75 & 2.625 \end{bmatrix}$$

$$\theta = \begin{bmatrix} 3 & 0 & 0 & 0 & 0 & 0 \\ 0 & 3 & 0 & 0 & 0 & 0 \\ 0 & 0 & 3 & 0 & 0 & 0 \\ 0 & 0 & 0 & 3 & 0 & 0 \\ 0 & 0 & 0 & 0 & 3 & 0 \\ 0 & 0 & 0 & 0 & 0 & 3 \end{bmatrix}$$

where $\lambda_{max}(\eta) = 8.8, \lambda_{min}(\eta) = 0.5, \lambda_{min}(\theta) = 3, M = 1600, \|\eta\check{E}\| = 8.58$, according to (40), $\phi_{max} = 96k, x_{10}(0) = 0, x_1(0) = [-1, 2, 1], x_{20}(0) = 5, x_2(0) = [1.2, 1, 1.2], \psi = 2.46, \pi = 0.757, \epsilon = 2, k_0 = 1$.

Figure 4 shows the change of dynamic parameter k over time.

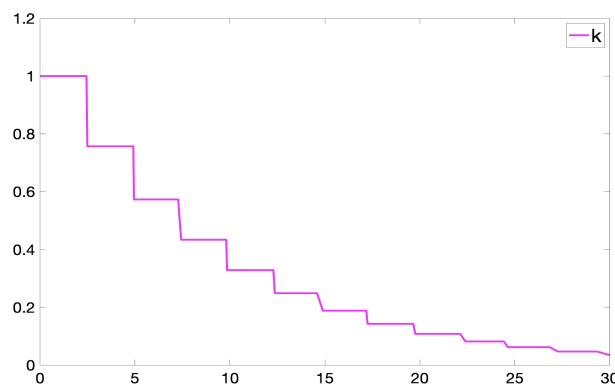


Figure 4. Zooming variable k .

The error of the novel adaptive dynamic quantizer is less than that of the dynamic uniform quantizer proposed in [25]. To show more clearly, we simplify the leader-following system as follows:

$$\begin{aligned} x_1 &= x_2 \\ x_2 &= q(u) \end{aligned} \tag{51}$$

where $q(u)$ is input quantized by quantizer, $x_1(0) = -1, x_2(0) = 1.2$, the parameters of the leader (11) and (12), the novel adaptive dynamic quantizer (6) and the dynamic uniform quantizer (4) are the same as those mentioned above. We get the error comparison between the two dynamic quantizers, as shown in Figure 5.

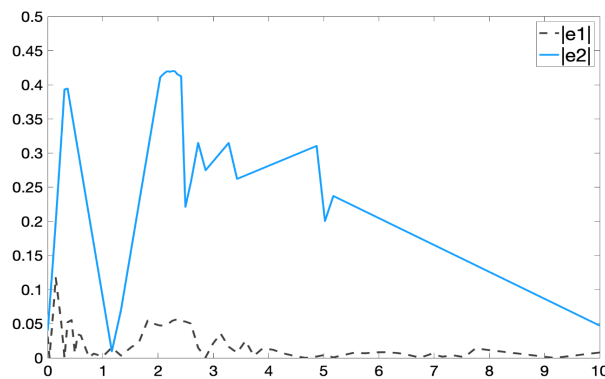


Figure 5. Dynamic quantizer quantization error.

Let $e1 = q_{\chi}(u) - u$, $e2 = q_{\mu}(u) - u$, $e1$ and $e2$ are the quantization errors under the action of the new adaptive dynamic quantizer and uniform quantizer [25], respectively. Figure 5 show the comparison between the quantization error of the newly proposed dynamic quantizer and the quantization error of the dynamic uniform quantizer in the system (51). These simulation results confirm that $e1 \leq 0.12$ and $e2 \leq 0.42$. Moreover, we can get the error of the novel dynamic quantizer at any time is less than dynamic uniform quantizer error.

The following is applied to the multi-agent system shown in Figure 3, where the follower’s input is quantized by the dynamic quantizer (6) proposed in this paper.

Figure 6 shows the speed of three followers hanging points. The final velocity tends to be 1.

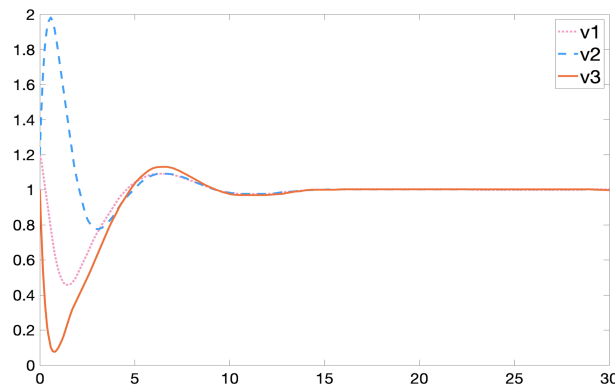


Figure 6. The Speed of Three Followers Hanging Points.

Figure 7 shows the errors between the speed of three followers’ hanging points and the speed of leaders’ hanging points. The final error tends to be 0.

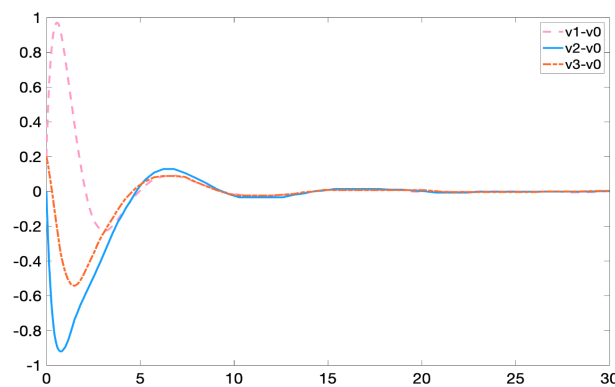


Figure 7. Errors between the Speed of Three Followers’ Hanging Points and the Speed of Leaders’ Hanging Points.

Figure 8 shows the errors between the displacement of three followers' hanging points and that of leaders' hanging points. The final error tends to be 0.

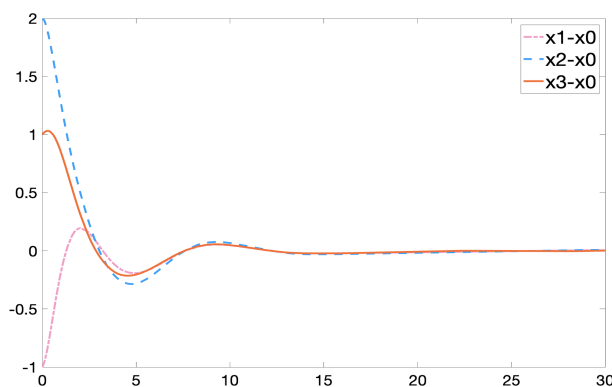


Figure 8. Errors between the displacement of three followers' hanging points and that of Leaders' hanging points.

Figure 9 shows the displacement of three followers' hanging points. Eventually followers and leaders' motion synchronization.

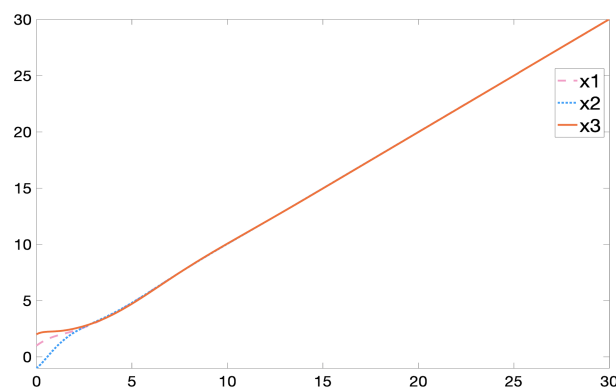


Figure 9. Displacement of Three Followers' Hanging Points.

6. Conclusions

In this paper, the novel adaptive dynamic quantizer combines the logarithmic quantizer and the uniform quantizer by introducing dynamic gain parameters. Under the same initial conditions, the quantization error of the newly proposed adaptive dynamic quantizer is less than or equal to 0.12, and the quantization error of the dynamic uniform quantizer is less than or equal to 0.42. From the above quantitative results, we get that the quantization error of the newly proposed adaptive dynamic quantizer is significantly smaller than the dynamic uniform quantizer. The final simulation proves that we solve the problem of leader-following consensus of second-order multi-agent systems after the follower input is quantized by the newly proposed adaptive dynamic quantizer.

Author Contributions: Authors H.S. and M.H. conceived and designed the model for research, analyzed the data and the obtained inference. Authors H.S. and M.H. processed data and wrote the paper. The final manuscript has been read and approved by all authors.

Funding: His research was funded by the The National Key R&D Plan, grant number 2017YFC0703903; The National Science Foundation of China, grant number 51705341, 51905357; Provincial Science Foundation of Liaoning, grant number 2019-ZD-0654.

Acknowledgments: The authors are grateful to the editors and the anonymous reviewers for providing us with insightful comments and suggestions throughout the revision process.

Conflicts of Interest: The authors declare no conflict of interest.

Appendix A

Appendix A.1. Proof of Identity (7)

When $k = 1$.

$$|u| < u_{th}$$

$$|\Delta q_\chi| = |q_\chi(|u|) - |u|| \leq \delta|u| + b \tag{A1}$$

where u is input, $0 < \delta < 1$, b is a constant, when $u = \frac{d}{1+\delta}$, we get $|\Delta q_\chi| = \frac{d}{1+\delta}$.

$$b = \frac{d(1-\delta)}{1+\delta} \leq d(1-\delta) \tag{A2}$$

The following inequalities are obtained by introducing (A2) into (A1).

$$|\Delta q_\chi| \leq \delta|u| + d(1-\delta) \tag{A3}$$

$$u_{th} \leq |u| \leq M$$

$$\begin{aligned} |\Delta q_\chi| &= |q_\chi(|u|) - |u|| \\ &\leq \left(\frac{|u|}{\omega} + \frac{1}{2}\right)\omega - |u| \\ &= \frac{1}{2}\omega \end{aligned} \tag{A4}$$

When we bring in the dynamic parameter k , the error of the new dynamic quantizer is as follows.

$$|u| < ku_{th}$$

According to (6) and (A3), we get

$$\begin{aligned} |\Delta q_\chi| &= |kq_\chi\left(\frac{|u|}{k}\right) - |u|| \\ &= \left|kq_\chi\left(\frac{|u|}{k}\right) - k\frac{|u|}{k}\right| \\ &= k|\Delta q_x\left(\frac{|u|}{k}\right)| \leq k\left(\delta\frac{|u|}{k} + d(1-\delta)\right) \end{aligned} \tag{A5}$$

$$ku_{th} \leq |u| \leq kM$$

According to (6) and (A4), we get

$$\begin{aligned} |\Delta q_\chi| &= |kq_\chi\left(\frac{|u|}{k}\right) - |u|| \\ &\leq \left(\frac{|u|}{k\omega} + \frac{1}{2}\right)k\omega - |u| \\ &= \frac{1}{2}k\omega \end{aligned} \tag{A6}$$

Appendix A.2. The Solution Process of T^+

To solve the pseudo inverse of T matrix, T is divided into the following forms of BC multiplication.

$$T = BC \tag{A7}$$

The actual values of B and C matrices are as follows.

$$B = \begin{bmatrix} 1 & 0 & \cdots & 0 \\ 1 & 1 & \cdots & 0 \\ \vdots & \vdots & \ddots & \vdots \\ 1 & 1 & \cdots & 1 \end{bmatrix}$$

$$C = \begin{bmatrix} -1 & 1 & \cdots & 0 \\ 0 & -1 & \cdots & 0 \\ 0 & 0 & \cdots & 0 \\ \vdots & \vdots & \ddots & \vdots \\ 0 & 0 & \cdots & 1 \end{bmatrix}$$

where $B \in R^{N \times N}$ and $C \in R^{N \times N}$, according to the solution formula of generalized inverse matrix, T^+ is transformed into the following form.

$$T^+ = C^H(CC^H)^{-1}(B^HB)^{-1}B^H \tag{A8}$$

References

1. Shen, Y.; Kong, Z.; Ding, L. Flocking of Multi-Agent System with Nonlinear Dynamics via Distributed Event-Triggered Control. *Appl. Sci.* **2019**, *9*, 1336.
2. Zhang, W.; Liu, J. Ultra-fast consensus of discrete-time multi-agent systems under a unified framework. *Int. J. Control* **2015**, *88*, 1123–1132.
3. Li, R. Leader-Following Output Synchronization for a Class of Uncertain Nonlinear Multi-Agent Systems Under Uniformly Connected Network. *Asian J. Control* **2015**, *17*, 1924–1934.
4. Pan, L.; Lu, Q.; Yin, K.; Zhang, B. Signal Source Localization of Multiple Robots Using an Event-Triggered Communication Scheme. *Appl. Sci.* **2018**, *8*, 977–999.
5. Li, R.; Yang, G. Consensus Control of a Class of Uncertain Nonlinear Multiagent Systems via Gradient-Based Algorithms. *IEEE Trans. Cybern.* **2019**, *49*, 2085–2094.
6. Zhang, W.; Liu, J. Consensusability of multi-agent systems via multi-order relative output derivative feedback. In Proceedings of the 11th World Congress on Intelligent Control and Automation, Shenyang, China, 29 June–4 July 2014.
7. Liu, W.; Huang, J. Adaptive Leader-Following Consensus for a Class of Nonlinear Multi-Agent Systems with Jointly Connected Switching Networks. *Automatica* **2017**, *79*, 84–92.
8. Lu, M.; Lu, L. Leader-Following Consensus of Multiple Uncertain Euler-Lagrange Systems Subject to Communication Delays and Switching Networks. *IEEE Trans. Autom. Control* **2018**, *63*, 2604–2611.
9. Xu, X.; Liu, L.; Feng, G. Consensus of Discrete-Time Linear Multi-Agent Systems With Communication, Input and Output Delays. *IEEE Trans. Autom. Control* **2018**, *62*, 492–497.
10. Yu, Z.; Liu, Y.; Wen, G.; Chen, G. Distributed Optimization of Linear Multi-Agent Systems: Edge- and Node-Based Adaptive Designs. *IEEE Trans. Autom. Control* **2017**, *62*, 3602–3609.
11. Park, M.-J.; Kwon, O.-M.; Seuret, A. Weighted Consensus Protocols Design Based on Network Centrality for Multi-Agent Systems With Sampled-Data. *IEEE Trans. Autom. Control* **2017**, *62*, 2916–2922.
12. Zhu, W.; Jiang, Z. Event-Based Leader-Following Consensus of Multi-Agent Systems with Input Time Delay. *IEEE Trans. Autom. Control* **2015**, *60*, 1362–1367.
13. Shao, J.; Zheng, W.X.; Huang, T.-Z.; Bishop, A.N. On Leader-Follower Consensus with Switching Topologies: An Analysis Inspired by Pigeon Hierarchies. *IEEE Trans. Autom. Control* **2018**, *63*, 3588–3593.
14. Liu, W.; Huang, J. Cooperative global robust output regulation for second-order nonlinear multi-agent systems with jointly connected switching networks. In Proceedings of the 2016 American Control Conference (ACC), Boston, MA, USA, 6–8 July 2016; pp. 1596–1601.
15. Li, R.; Hong, Y. Semi-global cooperative output regulation of a class of nonlinear uncertain multi-agent systems under switching networks. *Int. J. Robust Nonlinear Control* **2017**, *27*, 5061–5081.

16. Su, Y.; Huang, J. Cooperative Output Regulation of Linear Multi-Agent Systems. *IEEE Trans. Autom. Control* **2012**, *62*, 1248–1253.
17. Su, Y.; Huang, J. Cooperative Output Regulation with Application to Multi-Agent Consensus Under Switching Network. *IEEE Trans. Syst. Man Cybern. Part B (Cybern.)* **2012**, *42*, 864–875.
18. Carli, R.; Bullo, F.; Zampieri, S. Quantized average consensus via dynamic coding/decoding schemes. *Int. J. Robust Nonlinear Control* **2010**, *20*, 156–175.
19. De Candido, O.; Jemba, H.; Mezghani, A. Reconsidering Linear Transmit Signal Processing in 1-Bit Quantized Multi-User MISO Systems. *IEEE Trans. Wirel. Commun.* **2019**, *18*, 254–267.
20. Liu, T.; Huang, J. Adaptive Cooperative Output Regulation of Discrete-Time Linear Multi-Agent Systems by a Distributed Feedback Control Law. *IEEE Trans. Autom. Control* **2018**, *63*, 4383–4390.
21. Liu, M.; Xiong, J. Bilinear Transformation for Discrete-Time Positive Real and Negative Imaginary Systems. *IEEE Trans. Autom. Control* **2018**, *63*, 4264–4269.
22. Lichnerowicz, A. Deformation theory and quantization. *Lect. Notes Phys.* **1979**, *94*, 280–289.
23. Ma, J.; Ji, H.; Sun, D.; Feng, G. An approach to quantized consensus of continuous-time linear multi-agent systems. *Automatica* **2018**, *91*, 98–104.
24. Xing, L.; Wen, C.; Lei, W. Adaptive output feedback regulation for a class of nonlinear systems subject to input and output quantization. *J. Frankl. Inst.* **2017**, *354*, 6536–6549.
25. Zeng, Z.; Wang, X.; Zheng, Z.; Zhao, L. Edge agreement of second-order multi-agent system with dynamic quantization via the directed edge Laplacian. *Nonlinear Anal. Hybrid Syst.* **2017**, *23*, 1–10.
26. Yang, Z.; Hong, Y.; Jiang, Z.-P.; Wang, X. Quantized feedback stabilization of hybrid impulsive control systems. In Proceedings of the 48th IEEE Conference on Decision and Control (CDC) held jointly with 2009 28th Chinese Control Conference, Shanghai, China, 15–18 December 2009; pp. 3903–3908.
27. Zhang, Q.; Zhang, J.-F. Quantized Data-Based Distributed Consensus under Directed Time-Varying Communication Topology. *SIAM J. Control Optim.* **2013**, *51*, 332–352.
28. Su, Y.; Huang, J. Cooperative global output regulation of heterogeneous second-order nonlinear uncertain multi-agent systems. *Automatica* **2013**, *49*, 3345–3350.
29. Liu, W.; Huang, J. Cooperative Global Robust Output Regulation for Nonlinear Output Feedback Multi-Agent Systems Under Directed Switching Networks. *IEEE Trans. Autom. Control* **2017**, *62*, 6339–6352.
30. Xing, L.; Wen, C.; Zhu, Y.; Su, H.; Liu, Z. Output feedback control for uncertain nonlinear systems with input quantization. *Automatica* **2016**, *65*, 191–202.
31. Zhang, W.; Wang, H.; Liu, J. Multi-tracking control of heterogeneous multi-agent systems with single-input–single-output based on complex frequency domain analysis. *IET Control Theory Appl.* **2016**, *10*, 861–868.
32. Godsil, C.; Royle, G. *Algebraic Graph Theory*; Springer: New York, NY, USA, 2004.
33. Cai, K.; Ishii, H. Convergence time analysis of quantized gossip consensus on digraphs. *Automatica* **2012**, *48*, 2344–2351.
34. Qian, Y.; Cui, B.; Lou, X. Quantized feedback control for hybrid impulsive control systems. In Proceedings of the International Conference on Control, Automation and Systems, JeJu Island, Korea, 17–21 October 2012; pp. 3093–3098.
35. De Persis, C.; Mazenc, F. Stability of quantized time-delay nonlinear systems: A Lyapunov-Krasovskii functional approach. *Math. Control Signals Syst.* **2010**, *21*, 4337–4370.
36. Zhou, J.; Wen, C.; Yang, G. Adaptive backstepping stabilization of nonlinear uncertain systems with quantized input signal. *IEEE Trans. Autom. Control* **2018**, *59*, 460–464.
37. Hayakawa, T.; Ishii, H.; Tsumura, K. Adaptive quantized control for linear uncertain discrete-time systems. In Proceedings of the 2005 American Control Conference, Portland, OR, USA, 8–10 June 2005; pp. 4784–4789.
38. Ceragioli, F.; De Persis, C.; Frasca, P. Discontinuities and hysteresis in quantized average consensus. *Automatica* **2011**, *47*, 1916–1928.
39. Liu, T.; Jiang, Z.-P.; Hill, D.J. A sector bound approach to feedback control of nonlinear systems with state quantization. *Automatica* **2012**, *48*, 145–152.

40. Huang, J.; Chen, Z. A General Framework for Tackling the Output Regulation Problem. *IEEE Trans. Autom. Control* **2004**, *49*, 2203–2218.
41. Liberzon, D. Hybrid feedback stabilization of systems with quantized signals. *Automatica* **2003**, *39*, 1543–1554.



© 2019 by the authors. Licensee MDPI, Basel, Switzerland. This article is an open access article distributed under the terms and conditions of the Creative Commons Attribution (CC BY) license (<http://creativecommons.org/licenses/by/4.0/>).